


# Design and simulation of AlN-based vertical Schottky barrier diodes

Chun-Xu Su(苏春旭), Wei Wen(温暐), Wu-Xiong Fei(费武雄), Wei Mao(毛维), Jia-Jie Chen(陈佳杰), Wei-Hang Zhang(张苇杭), Sheng-Lei Zhao(赵胜雷), Jin-Cheng Zhang(张进成), and Yue Hao(郝跃)

**Citation:**Chin. Phys. B, 2021, 30 (**6**): 067305. DOI: 10.1088/1674-1056/abe0c7

Journal homepage: http://cpb.iphy.ac.cn; http://iopscience.iop.org/cpb

**What follows is a list of articles you may be interested in**

---

## Device topological thermal management of $\beta$-$Ga_2O_3$ Schottky barrier diodes

Yang-Tong Yu(俞扬同), Xue-Qiang Xiang(向学强), Xuan-Ze Zhou(周选择), Kai Zhou(周凯), Guang-Wei Xu(徐光伟), Xiao-Long Zhao(赵晓龙), and Shi-Bing Long(龙世兵)

Chin. Phys. B, 2021, 30 (**6**): 067302. DOI: 10.1088/1674-1056/abeee2

## Modeling, simulations, and optimizations of gallium oxide on gallium-nitride Schottky barrier diodes

Tao Fang(房涛), Ling-Qi Li(李灵琪), Guang-Rui Xia(夏光睿), and Hong-Yu Yu(于洪宇)

Chin. Phys. B, 2021, 30 (**2**): 027301. DOI: 10.1088/1674-1056/abc0dd

## Fabrication and characterization of vertical GaN Schottky barrier diodes with boron-implanted termination

Wei-Fan Wang(王伟凡), Jian-Feng Wang(王建峰), Yu-Min Zhang(张育民), Teng-Kun Li(李腾坤), Rui Xiong(熊瑞), Ke Xu(徐科)

Chin. Phys. B, 2020, 29 (**4**): 047305. DOI: 10.1088/1674-1056/ab7909

## A simulation study of field plate termination in $Ga_2O_3$ Schottky barrier diodes

Hui Wang(王辉), Ling-Li Jiang(蒋苓利), Xin-Peng Lin(林新鹏), Si-Qi Lei(雷思琦), Hong-Yu Yu(于洪宇)

Chin. Phys. B, 2018, 27 (**12**): 127302. DOI: 10.1088/1674-1056/27/12/127302

## Performance of $La_2O_3$/InAlN/GaN metal–oxide–semiconductor high electron mobility transistors

Feng Qian, Li Qian, Xing Tao, Wang Qiang, Zhang Jin-Cheng, Hao Yue

Chin. Phys. B, 2012, 21 (**6**): 067305. DOI: 10.1088/1674-1056/21/6/067305

---

# Design and simulation of AlN-based vertical Schottky barrier diodes*

Chun-Xu Su(苏春旭)[1], Wei Wen(温暐)[2], Wu-Xiong Fei(费武雄)[2], Wei Mao(毛维)[1], Jia-Jie Chen(陈佳杰)[3], Wei-Hang Zhang(张苇杭)[1,†], Sheng-Lei Zhao(赵胜雷)[1], Jin-Cheng Zhang(张进成)[1,‡], and Yue Hao(郝跃)[1]

[1] *Key Laboratory of Wide Band-Gap Semiconductors and Devices, School of Microelectronics, Xidian University, Xi'an* 710071, *China*
[2] *China Electronic Product Reliability and Environmental Testing Research Institute, Guangzhou* 510610, *China*
[3] *Shanghai Academy of Spaceflight Technology, Shanghai* 201109, *China*

(Received 20 November 2020; revised manuscript received 6 January 2021; accepted manuscript online 28 January 2021)

The key parameters of vertical AlN Schottky barrier diodes (SBDs) with variable drift layer thickness (DLT) and drift layer concentration (DLC) are investigated. The specific on-resistance ($R_{on,sp}$) decreased to 0.5 m$\Omega\cdot$cm$^2$ and the breakdown voltage ($V_{BR}$) decreased from 3.4 kV to 1.1 kV by changing the DLC from $10^{15}$ cm$^{-3}$ to $3\times10^{16}$ cm$^{-3}$. The $V_{BR}$ increases from 1.5 kV to 3.4 kV and the $R_{on,sp}$ also increases to 12.64 m$\Omega\cdot$cm$^2$ by increasing DLT from 4-μm to 11-μm. The $V_{BR}$ enhancement results from the increase of depletion region extension. The Baliga's figure of merit (BFOM) of 3.8 GW/cm$^2$ was obtained in the structure of 11-μm DLT and $10^{16}$ cm$^{-3}$ DLC without FP. When DLT or DLC is variable, the consideration of the value of BFOM is essential. In this paper, we also present the vertical AlN SBD with a field plate (FP), which decreases the crowding of electric field in electrode edge. All the key parameters were optimized by simulating based on Silvaco-ATLAS.

**Keywords:** aluminum nitride, Schottky barrier diodes, specific on-resistance $R_{on,sp}$, breakdown voltage $V_{BR}$

**PACS:** 73.61.Ey, 73.30.+y, 51.50.+v **DOI:** 10.1088/1674-1056/abe0c7

## 1. Introduction

Owing to high breakdown voltage, ultralow conduction loss and high switching speed, GaN SBDs, have aroused great research interest in recent years.[1–6] Edge termination techniques, such as guard rings, field plate (FP) and ion implantation treatment, are introduced in vertical GaN SBDs to minimize field crowding and increase the reverse breakdown voltage ($V_{BR}$).[7–10] The $V_{BR}$ of vertical GaN SBDs has been enhanced from 300 V to 1650 V by using argon ion implantation.[11] For quasi-vertical GaN-based SBDs, on/off current ratio of $10^{10}$ and average breakdown electric field of 1.48 MV/cm were obtained by improving material design and device fabrication process.[12,13] Due to the limited thickness of GaN drift layer, $V_{BR}$ is difficult to exceed 2000 V, and vertical GaN SBDs cannot be used in ultra-high voltage applications.

Aluminum nitride (AlN) materials possess high bandgap energy of 6.1 eV and high critical electric field of up to 12 MV/cm, demonstrating great potential in power electronics.[14] The improvement in quality of bulk AlN material has promoted the development of AlN SBDs. The lateral AlN SBDs with $V_{BR}$ of 1 kV has been reported, but the current density is below 1 A/cm$^2$.[15] Compared with lateral AlN SBDs, vertical AlN SBDs have the advantage of high current density. The $V_{BR}$ ranged from 550 V to 770 V for vertical AlN SBDs grown by hydride vapor phase epitaxy.[16] There are only a few studies on vertical AlN SBDs so far. The reported $V_{BR}$ and average breakdown electric field of AlN SBDs are all below 1 kV and 1 MV/cm respectively, which are far below the ideal material limit. Therefore, it is necessary to study the breakdown mechanism and device design of AlN SBDs.

In this paper, the vertical AlN SBDs was simulated by Silvaco-ATLAS. The thickness and doping concentration of the drift layer were employed to modulate $V_{BR}$ and $R_{on,sp}$ of the SBDs. This paper focus on the optimization of DLC and DLT to improve the *I*–*V* characteristics. The $V_{BR}$ is increased by 70%, which a FP is introduced at a specific concentration and thickness of drift layer for comparison.

## 2. Device structure

The simulated device of vertical AlN SBD as shown in Fig. 1. The Ni metal is utilized to form the Schottky contact electrode. The FP with a length of 0.5-μm are designed as shown in Fig. 1, which can increase the breakdown voltage by changing the degree of bending near the boundary of the depletion layer of the anode edge and changing the electric field distribution in the depletion layer. The SBD structure includes a 1-μm n+ AlN substrate and a drift layer with variable thickness. The substrate's concentration is assumed to be $10^{20}$ cm$^{-3}$, and its thickness is 1-μm. The drift layers with

*Project supported by Key-Area Research and Development Program of Guangdong Province, China (Grant Nos. 2020B010174001 and 2020B010171002) and Ningbo Science and Technology Innovation 2025 (Grant No. 2019B10123).
†Corresponding author. E-mail: whzhang@xidian.edu.cn
‡Corresponding author. E-mail: jchzhang@xidian.edu.cn
© 2021 Chinese Physical Society and IOP Publishing Ltd 

different DLTs (4 μm, 5 μm, 6 μm, 8 μm, 11 μm) are simulated. In the structure with a variable DLC, we change it from $1\times10^{15}$ cm$^{-3}$ to $3\times10^{16}$ cm$^{-3}$, while the DLT is 11-μm. The material of SiN is used for passivation layer. In the structure of vertical GaN SBD, the DLC is $10^{16}$ cm$^{-3}$, the thickness of drift layer is 11-μm, other parameters are consistent with AlN SBDs. The SBDs were simulated by Silvaco-ATLAS. The ionized charge in the drift layer was assumed to be uniform.

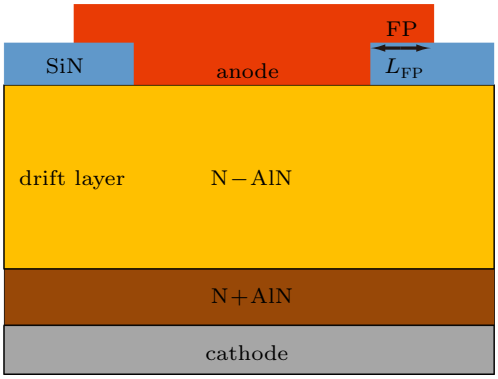



**Fig. 1.** The device structure of the vertical AlN-based SBD with FP.

## 3. Results and discussion

As shown in Fig. 2(a), the vertical AlN and GaN SBDs are simulated. The $V_{on}$ is defined at the point when the current density is 1 A/cm$^2$. Compared with GaN SBDs, the forward turn-on voltage ($V_{on}$) of AlN SBDs is increased from 0.5 V to 3.1 V due to the lower electron affinity energy. A relation about the height of Schottky barrier ($\Phi_B$) in n-type semiconductor material is[17]

$$q\Phi_B = q\Phi_m - \chi_s, \tag{1}$$

where $\Phi_m$ is the work function of contact metal, $\chi_s$ is the electron affinity energy. Thus, the $q\Phi_B$ of AlN device is larger when the same contact metal is used that lead to the increase of $V_{on}$. As shown in Fig. 2(a), the extracted ideal factor(n) of AlN SBD and GaN SBD are 1.08 and 1.01, respectively. The extracted Schottky barrier heights form the *I*–*V* forward curve of the AlN SBD and GaN SBD are 3.45 eV and 0.74 eV, which are consistent with height extracted from the structure diagram in Silvaco tonyplot. The critical electric filed and breakdown voltage $V_{BR}$ are significantly improved for AlN material. The $V_{BR}$ is defined as the anode voltage at which the peak electric field reaches 12 MV/cm. As shown in Fig. 2(b), the critical electric field is improved from 3.3 MV/cm to 12 MV/cm, and the corresponding breakdown voltage is improved from −300 V to −2300 V.

As shown in Fig. 3, vertical AlN SBDs with various DLTs are simulated. Figure 3(a) shows the forward *I*–*V* characteristics of the SBDs with different DLTs. We can see that the lager the DLT is, the smaller the current density is. The decrease of current density is primarily due to the reduction of available charge carriers in the thick drift-layer thus resulting in the increased series resistance.[18] As shown in Fig. 3(b), the peak electric field decreases with the increase of DLT at the same voltage of −1800 V. Figure 3(c) shows the electric field distribution in vertical direction at the voltage of −1800 V. From Fig. 3(d), we can see the $V_{BR}$ and $R_{on,sp}$ increased with the increase of DLT.

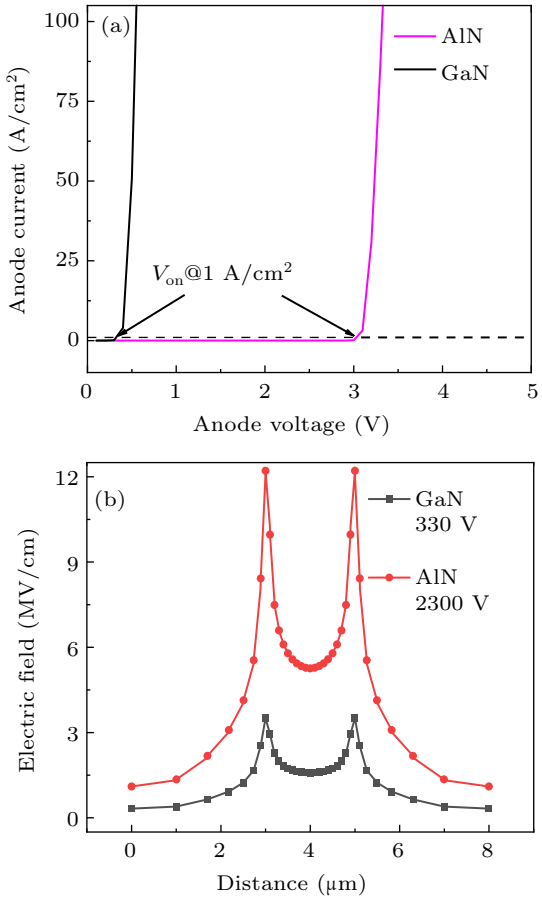



**Fig. 2.** Comparison of vertical AlN SBDs and GaN SBDs without FP. (a) The diagram of forward bias *I*–*V* characteristics. (b) The diagram of electric field distribution at 10 nm below the anode.

The impact of DLC on forward and reserve *I*–*V* characteristic is shown in Fig. 4. Figure 4(a) shows the forward *I*–*V* characteristic which become better with the increase of the DLC. From Fig. 4(b), we can see that the $V_{BR}$ decreases which from −3.37 kV to −1.1 kV with the increased DLC. The $V_{BR}$ is inversely proportional to the doping concentration. The electric field decreases to zero at the boundary of drift layer in the SBDs with four gradients of DLC from $1\times10^{15}$ cm$^{-3}$ to $1\times10^{16}$ cm$^{-3}$, nevertheless in DLC of $3\times10^{16}$ cm$^{-3}$, the electric field rapidly fell to zero at the distance of 5 μm away from anode, that means the thickness of depletion layer is about 5 μm.

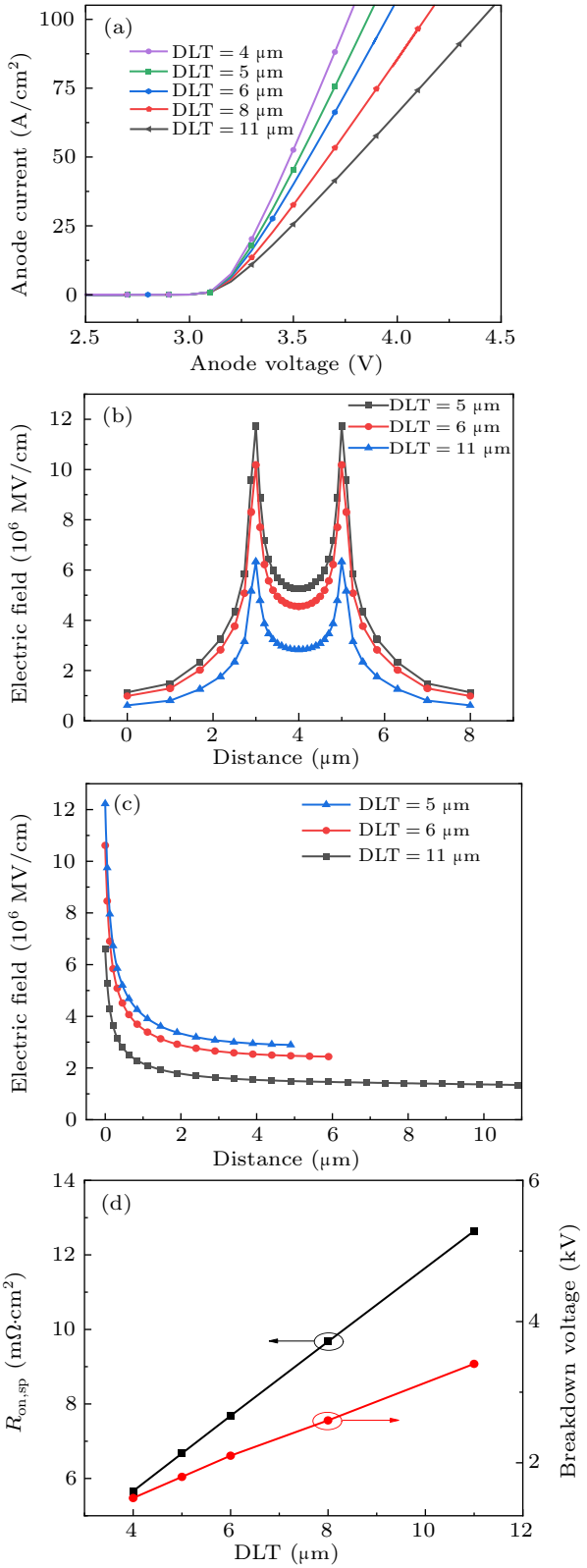



**Fig. 3.** The diagram of (a) forward *I*–*V* characteristics of vertical AlN SBDs with different DLTs, (b) electric field distribution at 10 nm below the anode, (c) electric field distribution along the vertical direction for the devices with different DLTs, (d) $V_{BR}$ and $R_{on}$ as a function of DLT.

At the boundary of the depletion region, the electric field is zero, the electric field distribution function of the depletion region is[17]

$$E(x) = -\frac{qN_D}{\varepsilon_S}(W_D - x). \tag{2}$$

From Fig. 4(b), we can see the maximum of electric field $E_m$ appears at the interface of the metal and semiconductor. The potential distribution equation

$$V(x) = \frac{qN_D}{\varepsilon_S}(W_D x - \frac{x^2}{2}). \tag{3}$$

The potential at the boundary of the depletion region has the following relationship with the applied reverse bias:

$$V(W_D) = V_a. \tag{4}$$

Thus, the maximum electric field is $E_m = 2qN_D V_a/\varepsilon_S$. When $E_m$ is equal to critical electric field of AlN (12 MV/cm),$V_a$ is inversely proportional to $N_D$, so the $V_{BR}$ decreased with the DLC increase. From $W_D = 2\varepsilon_S V_a/qN_D$, we can see the $W_D$ decreased with the DLC increase. And the diagram of electron concentration distribution is shown in Fig. 4(c), which indicated that the drift layer is not completely depleted because of the high DLC.

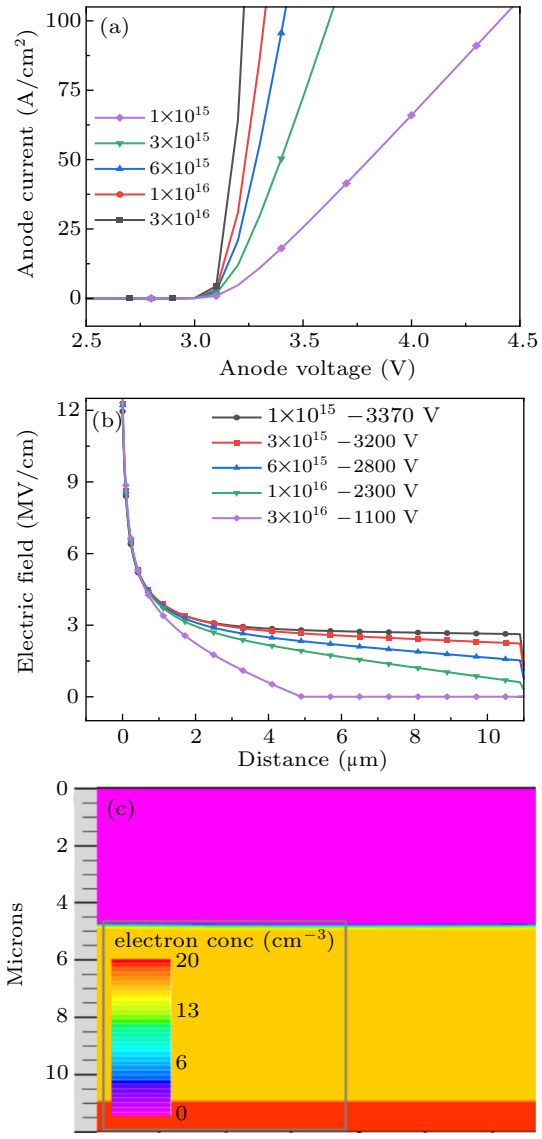



**Fig. 4.** The diagram of (a) forward *I*–*V* characteristics of vertical AlN SBDs with different DLCs, (b) electric field distribution along the vertical direction for the devices with different DLCs, (c) electron concentration schematics of the device with DLC of $3 \times 10^{16}$ cm$^{-3}$.

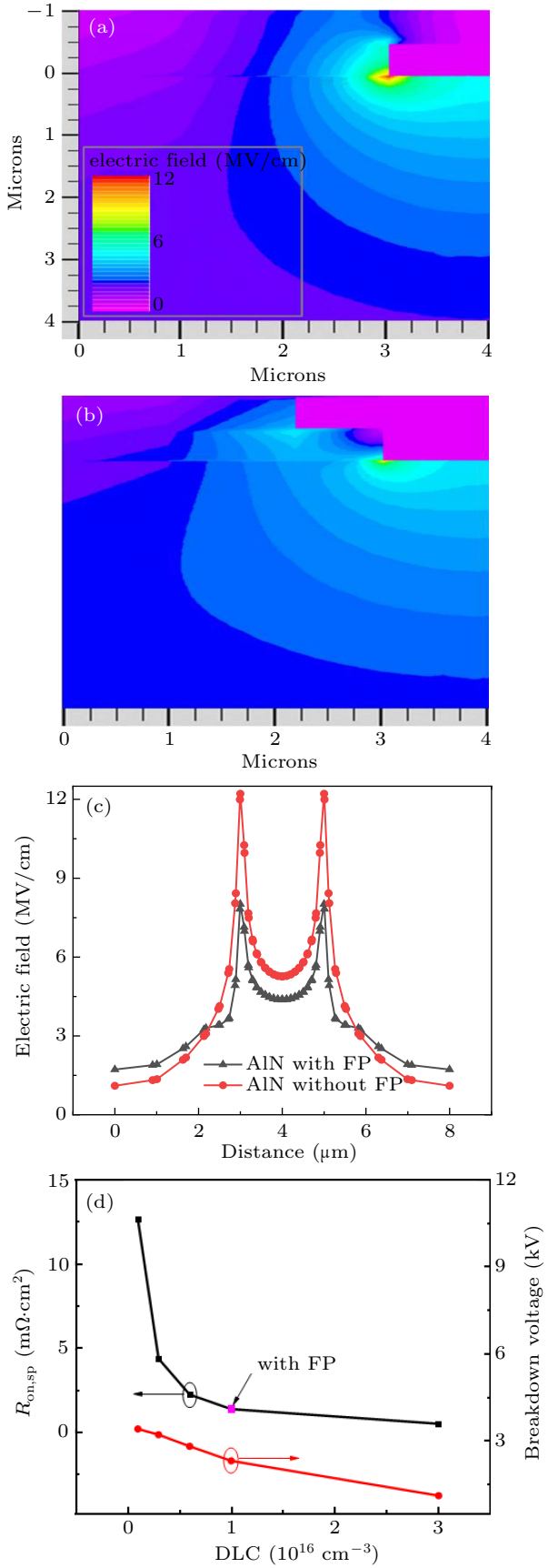



**Fig. 5.** The diagram of (a) electric field without and (b) with FP, (c) electric field distribution at 10 nm below the anode ($V_{anode} = -2300$ V), (d) $V_{BR}$ and $R_{on}$ as a function of DLC.

Figure 5 shows the comparison between the structure with and without FP. From Figs. 5(a) and 5(b), we can see that the electric field crowding is reduced in the structure with FP. At the same anode voltage of −2300 V. The electric filed peak is reduced from 12 MV/cm to 8 MV/cm by utilizing field plate which is shown in Fig. 5(c). Figure 5(d) is the dual coordinate diagram of A and B about DLC, the $V_{BR}$ of AlN SBDs is further increased from −2300 V to −4100 V.

As shown in Fig. 6(a), the value of BFOM increases from 397 MW/cm$^2$ to 914 MW/cm$^2$ with the increase of DLT from 4 μm to 11 μm (the DLC is $1 \times 10^{15}$ cm$^{-3}$). From Fig. 6(b), we can see that BFOM increases for DLC $< 1 \times 10^{16}$ cm$^{-3}$ and decreases for DLC $> 1 \times 10^{16}$ cm$^{-3}$. The maximum BFOM can be obtained from a simulation of $V_{BR}$ as a function of DLC. In this paper, we obtain a maximum BFOM of 12.3 GW/cm$^2$ in the simulation of the structure with FP, which is 3 times of the BFOM compared with the structure without FP under the same DLC and DLT.

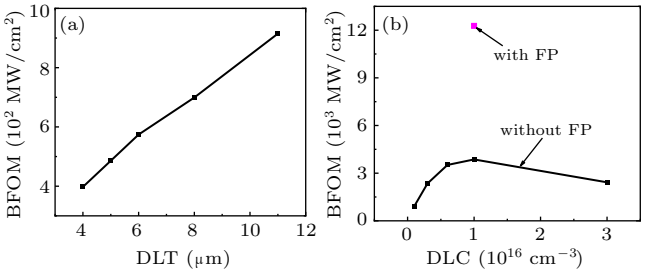



**Fig. 6.** BFOM as a function of (a) DLT and (b) DLC include the structure with FP.

## 4. Conclusion

In summary, the evaluations of drift layer's thickness and doping concentration on *I*–*V* characteristics for vertical AlN Schottky barrier diodes are investigated by simulation. The lager DLT is essential to improve the $V_{BR}$ and BFOM effectively. For the SBD with DLT of 11-μm, the $V_{BR}$ can reach −3400 V. The forward *I*–*V* characteristics can be improved by increasing the drift layer's doping concentration. By increasing the DLC, the $R_{on,sp}$ is further decreased from 12.64 mΩ · cm$^2$ to 0.5 mΩ·cm$^2$, but the effect of this method to improve $V_{BR}$ is adverse. The devices with lager doping concentrations are more likely to cause carrier multiplication when they are subjected to reverse bias. Thus, the combined effect of $V_{BR}$ and $R_{on,sp}$ should be considered comprehensively to obtain a higher BFOM value. The vertical AlN SBD with FP also been simulated to improve $V_{BR}$ in this paper. Besides these methods, many other devices with termination structures are used to improve *I*–*V* characteristics in vertical SBDs, which can be introduced in our paper.

At present, the existing experimental level of the AlN vertical SBD had a lot of material defects,[16] resulting in a small forward current density, and the ideal factor ($n$) was about 8. The high value of $n$ indicated that the transport mechanism deviates from the thermionic emission (TE) model,

which is mainly caused by the nonuniform contact at the metal/semiconductor interface due to material defects. The calculated resistivity of $2.3 \times 10^2\ \Omega \cdot \mathrm{cm}$, suggesting that the carrier concentration of the active region was low. As a result, it is highly desired to decrease the defect density of AlN epitaxial layers. In this paper, the simulated AlN vertical SBD suggests that high quality of material as a precondition to great potential of vertical AlN power devices.

## References


[1] Kuzmik J 2001 *IEEE Electron Device Lett.* **22** 510

[2] Palacios T, Chakraborty A, Rajan S, Poblenz C, Keller S, Denbaars S P, Speck J S and Mishra U K 2005 *IEEE Electron Device Lett.* **26** 781

[3] Lee J G, Park B R, Cho C H, Seo K S and Cha H Y 2013 *IEEE Electron Device Lett.* **34** 214

[4] Zhou Q, Jin Y, Shi Y Y, Mou J Y, Bao X, Chen B W and Zhang B 2015 *IEEE Electron Device Lett.* **36** 660

[5] Zhou Q, Yang Y, Hu K, Zhu R P, Chen W J and Zhang B 2017 *IEEE Transactions on Industrial Electronics.* **64** 8971

[6] Wang H, Kwan A M H, Jiang Q and Chen K J 2015 *IEEE Trans. Electron Devices* **62** 1143

[7] Horii T, Miyazaki T, Saito Y, Hashimoto S, Tanabe T and Kiyama M 2009 *Materials Science Forum.* **615–617** 963

[8] Saitoh Y, Sumiyoshi K, Okada M, Horii T and Nakamura T 2013 *Appl. Phys. Express* **3** 081001

[9] Lei Y, Shi H, Lu H, Chen D, Zhang R and Zheng Y 2013 *J. Semicond.* **34** 054007

[10] Tanaka N, Hasegawa K, Yasunishi K, Murakami N and Oka T 2015 *Appl. Phys. Express* **8** 071001

[11] Ozbek A M and Baliga B J 2011 *IEEE Electron Device Lett.* **32** 300

[12] Li Y, Shen B, Wang M, Yin R, Zhang J, Tao M and Wen C P 2020 *IEEE Electron Device Lett.* **41** 329

[13] Bian Z K, Zhang J C, Zhao S L, Zhang Y C and Hao Y 2020 *IEEE Electron Device Lett.* **41** 1476

[14] Irokawa Y, Villora E A G and Shimamura K 2012 *J. Appl. Phys.* **51** 040206

[15] Fu H, Baranowski I, Huang X, Chen H, Lu Z and Montes J 2017 *IEEE Electron Device Lett.* **38** 1286

[16] Kinoshita T, Nagashima T, Obata T, *et al.* 2015 *J. Appl. Phys.* **8** 061003

[17] Baliga B J 2008 *Fundamentals of Power Semiconductor Devices* pp. 96–97, 171

[18] Sandupatla A, Arulkumaran S, Ng G I, Ranjan K, Deki M, Nitta S, Honda Y and Amano H 2019 *AIP Adv.* **9** 045007